Available online at www.sciencedirect.com

ScienceDirect

materialstoday: PROCEEDINGS

Materials Today: Proceedings 1S (2014) 109 – 121

Living Light: Uniting biology and photonics – A memorial meeting
in honour of Prof Jean-Pol Vigneron

Thin film and multilayer optics cause structural colors of many insects and birds

Doekele G. Stavenga[a,*]

[a]*Computational Physics, Zernike Institute for Advanced Materials, University of Groningen, NL-9747 AG Groningen, the Netherlands*

Abstract

Structural effects contribute to the coloration of many animals. Whereas extremely complex structures have evolved, often coloration is due to the most simple structure, namely a thin film. Here we present a number of examples where thin film optics plays a prominent role, namely in insect wings and bird feathers. Most butterfly wing scales have a lower lamina that prominently determines the color. Damselfly wings with protrusions have reduced thin film reflections. A limited stack of multilayers features also distinct thin film properties, as is shown for feather barbules of the bird of paradise, Lawes' parotia. A simple method to derive the thickness of the wing structures is described.

© 2014 The Authors. Published by Elsevier Ltd. This is an open access article under the CC BY-NC-ND license
(http://creativecommons.org/licenses/by-nc-nd/3.0/).
Selection and Peer-review under responsibility of Physics Department, University of Namur.

Keywords: Butterfly wing scales, microspectrophotometry, scatterometry, barbules, melanin

1. Introduction

The living world is full of colors, playing often important roles in signaling and communication. Commonly colors in nature are attributed to light-absorbing pigments, but of course coloration due to regularly structured materials is also widely present. In fact, in many animals pigments and periodic structures are combined to optimize the reflection or transmission in very specific spectral ranges [1–4].

Figure 1 summarizes how pigments and structures can determine coloration. An unpigmented, randomly-structured material spatially scatters light of all wavelengths diffusely and thus is matt white [5]. Adding a pigment creates a diffuse pigmentary color. A medium that is periodically structured with submicrometer dimensions scatters light directionally, depending on the light wavelength, and thus becomes iridescent. Thin films are the most common cause of structural coloration, but multilayers occur also frequently, and several insect species have three-dimensional photonic crystals (3D PCs). Additional pigments cause spectrally filtered structural coloration [6,7]. Here we will

* Corresponding author. Tel.: +31-50-3634785
E-mail address: d.g.stavenga@rug.nl

2214-7853 © 2014 The Authors. Published by Elsevier Ltd. This is an open access article under the CC BY-NC-ND license
(http://creativecommons.org/licenses/by-nc-nd/3.0/).
Selection and Peer-review under responsibility of Physics Department, University of Namur.
doi:10.1016/j.matpr.2014.09.007

focus at a few exemplary cases of the most common structural arrangement causing structural coloration, namely the thin films and multilayers of insect wings and bird feathers.

The wings of insects consist of a thin membrane supported by a system of veins. In many insects, specifically flies, the wing membrane is very thin, with thickness $\leq 1\ \mu$m, but the wings are still sufficiently strong to enable agile flight due to the rather rigid venation. Due to thin film effects, the thin wing membranes can display a distinct coloration, which has been suggested to be important for intraspecific signaling [8]. The wing membranes of butterflies are normally invisible due to a dense coverage of wing scales. The wing scales are essentially flattened hair sacs and basically consist of two laminae connected by trabeculae, acting as pillars. The lower lamina is commonly about flat, with thickness ≈100-200 nm. The upper lamina is formed by an array of parallel ridges, with in between crossribs, thus leaving open windows for the scale interior. The distance between the ridges is in the order of 1 μm and the dimensions of the windows are even much less [9,10]. This basic architecture is often modified, however, and can be much more complex [1,2,6,7].

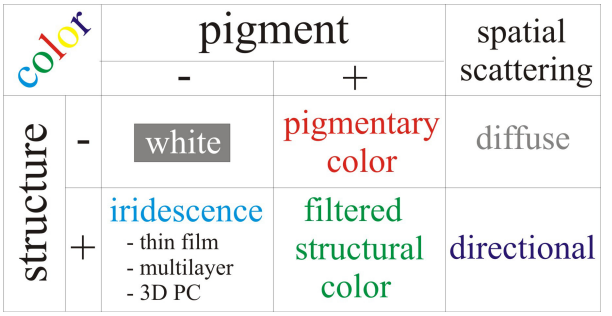

Fig. 1. Diagram for the interplay of the structure of materials and their pigmentation that determines the color. An unpigmented, randomly-structured material spatially scatters light of all wavelengths diffusely and thus is matt white. Adding a pigment creates a diffuse pigmentary color. A structured medium with submicrometer dimensions (a thin film, multilayer or three-dimensional photonic crystals) scatters light directionally and becomes iridescent. Additional pigments cause spectrally filtered structural coloration.

The wing scales of most butterflies are strongly pigmented and thus their color is fully attributed to their pigmentation. However, we recently discovered that the thin film optical properties of the lower lamina play a dominant role in tuning the color of most of the butterfly wing scales. The reflectance spectrum of the scales is firstly determined by the thickness of the lower lamina, and the pigment in lower and upper lamina subsequently acts as a spectral filter for the light reflected by the lower lamina. The general picture thus is that the reflectance of the lower lamina's thin film together with the absorbance spectrum of the pigment tune the scale color. In other words, the common butterfly wing scale combines structural with pigmentary coloration. Blue scales often appear to contain negligible amounts of pigment and the scale color is then fully structural [11,12].

Several butterfly species have scales with ridges consisting of stacks of lamellae acting as multilayers. The most famous examples are the intensely blue reflecting Morpho butterflies, but many pierids have scale ridges with essentially the same multilayer structure [13–16]. Depending on the layer thickness, the peak reflection can be iridescent blue or ultraviolet. The iridescent wing scales of pierids combine their structural coloration with diffuse pigmentary coloration [17,18].

The coloration of birds resides of course in their feathers. A bird feather consists of a main shaft and its many side branches, the barbs. Each barb in turn has numerous branches, the barbules. In the absence of pigment, the feathers are white, but melanins and other pigment classes usually create pigmentary coloration [19,20]. Structural coloration occurs when the feather barbs have a quasi-random, spongy structure, or when the barbules contain regularly arranged melanosomes, that is, melanized granules, rodlets or platelets, which are sometimes combined with regularly arranged air holes [21,22]. As before, pigments are added to structurally colored feathers to fine tune the feather coloration. Also in bird feathers, thin film and multilayer optics are dominant coloration mechanisms [23–25].

2. Materials and methods

2.1. Wings and feathers

An Andromica Clearwing butterfly, *Greta andromica*, was obtained from a commercial supplier. A mosquito (presumably *Culex pipiens*) and a Peacock butterfly were locally captured. Feathers from the bird-of-paradise *Parotia lawesii* were obtained from the Brisbane Natural History Museum. An American Rubyspot, *Hetaerina americana*, was obtained from the National Museum of Natural History Naturalis (Leiden, the Netherlands; curator Dr J. van Tol).

2.2. Spectrophotometry

Reflectance spectra were measured with a bifurcated probe (Avantes FCR- 7UV200; Avantes, Eerbeek, Netherlands), using an AvaSpec 2048-2 CCD detector array spectrometer (Avantes, Eerbeek, Netherlands). The light source was a deuterium-halogen lamp (AvaLight-D(H)-S). The bifurcated probe illuminated an area with a diameter of about 1 mm, and captured the light reflected in a small spatial angle. The spectra measured from directional reflecting surfaces were corrected for the diffusive properties of the white reference. Reflectance and transmittance spectra of wing areas were measured with an integrating sphere (AvaSphere-50-Refl) and the spectrometer, using a xenon light source. Reflectance and transmittance spectra of isolated scales were acquired with a microspectrophotometer (MSP), consisting of a xenon light source, a Leitz Ortholux microscope and an AvaSpec-2048 spectrometer (Avantes, Eerbeek, the Netherlands). The microscope objective was an Olympus 20x (NA 0.45). A white diffuse reference tile (Avantes WS-2) served as reference.

2.3. Reflectance and transmittance of a multilayer and a thin film

The reflectance and transmittance of a multilayer is conveniently calculated with a matrix formalism [26–28]. Consider a multilayer consisting of N infinite wide, thin layers of homogeneous dielectric media, separated by parallel surfaces, faced by media with (real) refractive indices n_0 and n_{N+1} (Fig. 2).

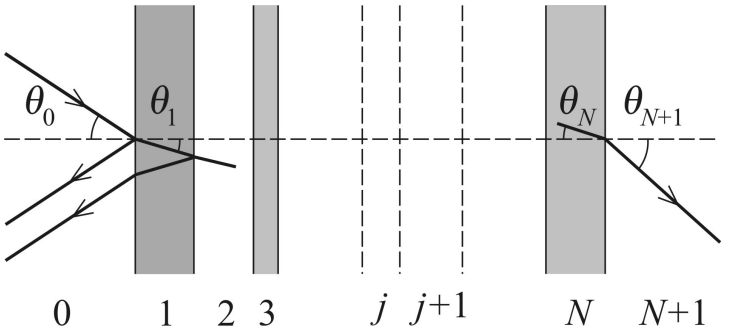

Fig. 2. Diagram of light propagation in a multilayer consisting of stack of N thin films with thickness d_j and refractive index n_j (j =1,2,...N) facing media with refractive indices n_0 and n_{N+1}. Incident light entering with an angle θ_0 to the normal, propagates in layer j with an angle θ_j, following from Snell's law.

The thicknesses of the layers are d_j and the refractive indices are in general complex: $n_j = n_{jR} - in_{jI}$ (j = 1, 2,..., N). The imaginary part of the refractive index is related to the absorption coefficient of the medium, κ_j, by $\kappa_j = 2kn_{jI}$, where $k = 2\pi/\lambda$ is the wave number in vacuum (λ is the light wavelength). The propagation of light through the multilayer is governed by Snell's law:

$$n_j \sin\theta_j = n_0 \sin\theta_0, \text{ with } j = 1, 2, ..., N + 1 \quad (1)$$

where the angle of incidence θ_j of the light ray at the interface of media j and $j+1$ can be complex. The light propagation through the multilayer is described by the transfer matrix

$$M = \begin{pmatrix} M_{11} & M_{12} \\ M_{21} & M_{22} \end{pmatrix} = D_0^{-1} \left[\prod_{j-1}^{N} Q_j \right] D_n \tag{2}$$

where

$$D_j = \begin{pmatrix} p_j & p_j \\ q_j & -q_j \end{pmatrix}, \text{ with } j = 1, 2, ..., N+1 \tag{3}$$

and

$$Q_j = \begin{pmatrix} a_j & ib_j p_j/q_j \\ ib_j q_j/p_j & a_j \end{pmatrix}, \text{ with } j = 1, 2, ..., N \tag{4}$$

with $a_j = \cos\phi_j$ and $b_j = \sin\phi_j$, where $\phi_j = kn_j d_j \cos\theta_j$. For TE-waves $p_j = 1$ and $q_j = n_j \cos\theta_j$, while for TM-waves $p_j = \cos\theta_j$ and $q_j = n_j$. The reflectance of the multilayer then is

$$R = \left| \frac{M_{21}}{M_{11}} \right|^2 \tag{5}$$

and the transmittance is

$$T = \frac{n_{N+1}}{n_0} \frac{\cos\theta_{N+1}}{\cos\theta_0} \left| \frac{1}{M_{11}} \right|^2 \tag{6}$$

For a single thin film, the reflectance is alternatively derived from $R = |r|^2$, where r is the reflection coefficient of the thin film, which is given for both TE- and TM-polarized light by the Airy formula [28,29]

$$r = \left(r_{01} + r_{12} e^{-2i\phi} \right) / \left(1 + r_{01} r_{12} e^{-2i\phi} \right) \tag{7}$$

where $\phi = kn_1 d \cos\theta_1$, $d = d_1$ is the thickness, and r_{01} and r_{12} are the reflection coefficients of the interfaces given by the Fresnel formulas:

$$\begin{aligned} \text{TE} \quad & r_{j-1,j} = (n_{j-1}c_{j-1} - n_j c_j)/(n_{j-1}c_{j-1} + n_j c_j) \\ \text{TM} \quad & r_{j-1,j} = (n_{j-1}c_j - n_j c_{j-1})/(n_{j-1}c_j + n_j c_{j-1}) \end{aligned} \tag{8}$$

with $j = 1, 2$; $c_j = \cos\theta_j$.

For the case where the refractive indices are real, the reflectance is (27-30)

$$R = \frac{r_{01}^2 + r_{12}^2 + 2r_{01}r_{12}\cos 2\phi}{1 + r_{01}^2 r_{12}^2 + 2r_{01}r_{12}\cos 2\phi} \tag{9}$$

The reflectance then has extrema (minima and maxima) for $\sin 2\phi = 0$, or, $\phi = u\pi/2$, with u > 0 and integer. For normal illumination ($\theta_j = 0$), the extrema thus occur for wavenumbers

$$k_{u1} = k_u n_1 = su \tag{10}$$

where $s = \pi/(2d)$ is the slope of the linear function of extremum wavenumber k_{u1} (in medium 1) and its number, u. The thickness of the thin film, d, hence can be derived from the slope:

$$d = u\lambda_u/(4n_1) = \pi/(2s) \tag{11}$$

In the common case that $n_1 > n_0, n_2$, the reflectance is maximal for u is odd and minimal for u is even. If $n_0 < n_1 < n_2$, the reflectance is maximal for u is even and minimal for u is odd.

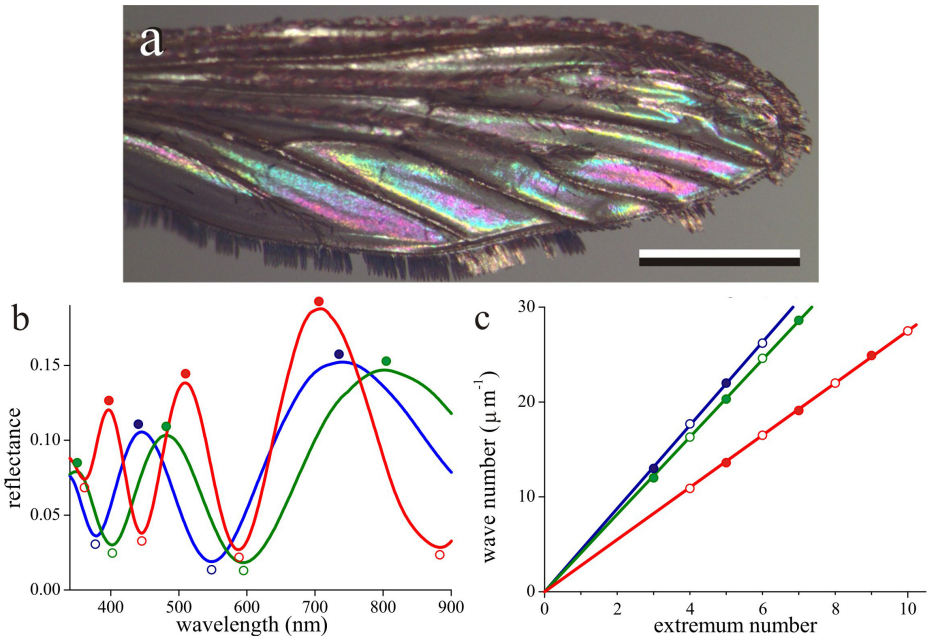

Fig. 3. Thin film optics of a wing of a mosquito. (a) The wing with clear venation showing distinct interference colours (scale bar: 1 mm). (b) Reflectance spectra of three different locations of the wing measured with a microspectrophotometer. (c) Wavenumbers of the reflectance extrema (closed symbol maxima; open symbols minima) fitted with a linear function.

3. Results

3.1. Mosquito wing membrane

Insect wings are generally thin and thus display structural colours. As an example, Figure 3a shows a wing of a mosquito. Observed with transmitted light, the wing is fully colourless, proving the absence of pigments, but with incident light, the wing membrane in between the veins features locally distinct colours, clearly indicating interference effects.

Reflectance spectra measured with a microspectrophotometer indeed have strong oscillations, characteristic for thin films (Fig. 3b). The wavelengths of the extrema, λ_e, indicated by the open and closed circles (Fig. 3b), yield the wave numbers of the extrema in vacuum, $k_e = 2\pi/\lambda_e$, and with the refractive index of insect cuticle, $n = A+B/\lambda^2$, with A = 1.517 and B = 8800 nm^2 ([19]; see Fig. 4a), the wave numbers of the extrema in the wing medium, k_{u1}, are obtained. The values thus derived for the three reflectance spectra of Figure 3b are well fitted by the linear function of Eq. 10. The local thicknesses of the wing then follow from the slopes of the linear fits, s, with $d = \pi/(2s)$, yielding 358, 385 and 571 nm, respectively (Fig. 3c: blue, green, red lines).

3.2. Butterfly wing membrane

Butterflies are generally much larger than flies, and accordingly the thickness of their wings may be expected to be also larger. Butterfly wings are usually fully covered by wing scales, but a clear exception is formed by the appropriately named clearwing (ithomiine) butterflies of the genus *Greta* (Fig. 4a, inset). Measurements with a bifurcated probe on wing areas void of scales of the Andromica Clearwing, *Greta andromica*, yield reflectance spectra with distinct oscillations, betraying thin film properties (Fig. 4b, blue curve). The wave numbers derived for the extrema combined with the wavelength-dependent wing refractive index (Fig. 4a), fit the linear function of Eq. 10 again very well (Fig. 4c), yielding a wing thickness of 730 nm. The full reflectance spectrum calculated for this thickness value with Eq. 9 shows indeed extrema at wavelengths closely corresponding to those of the measured spectrum (Fig. 4b, black curve). However, the modulation of the latter's spectrum is much smaller than 100%, and the

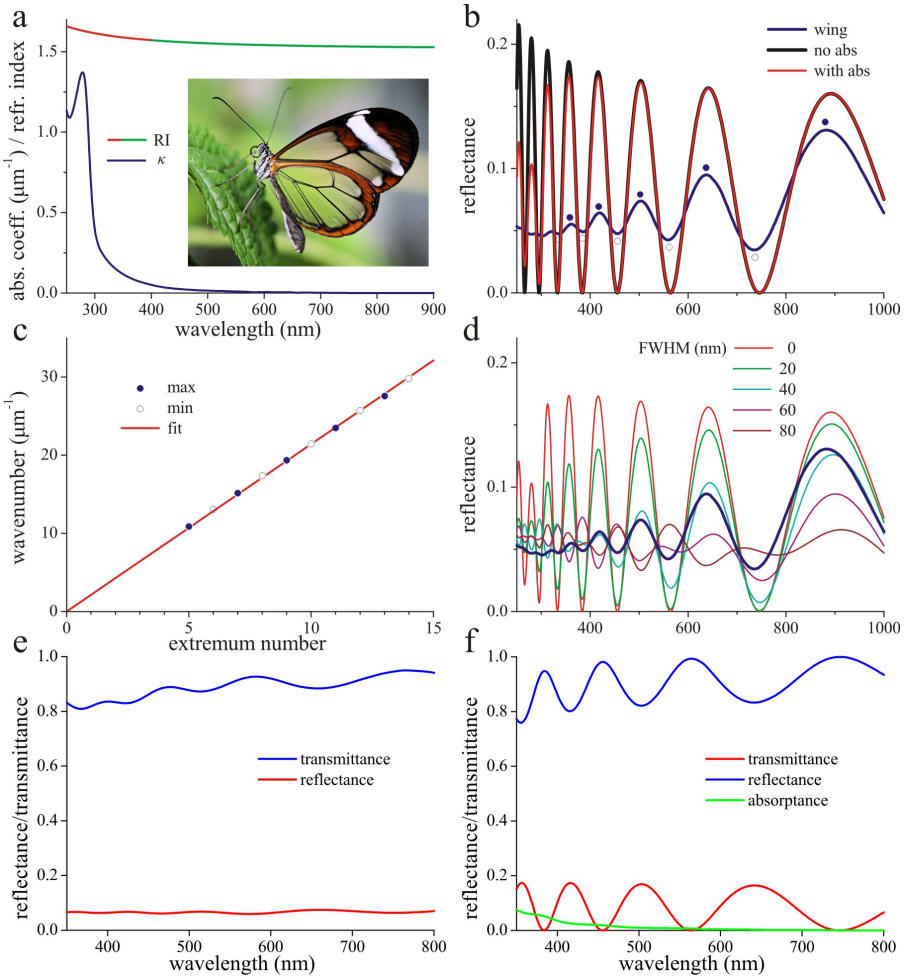

Fig. 4. Wing reflectance and transmittance of the Andromica Clearwing butterfly, *Greta andromica*. (a) Refractive index (RI) of insect cuticle given in the visible wavelength range by the function $n(\lambda) = 1.517+8800/\lambda^2$ (green curve, [19], extrapolated into the ultraviolet wavelength range (red curve), and absorption coefficient of insect cuticle, κ (blue curve); inset: photograph of the closely related *Greta oto*. (b) Reflectance spectrum measured with a bifurcated probe of the transparent part of the forewing of *G. andromica* (wing: blue curve; symbols indicate extrema), together with reflectance spectra calculated for a 730 nm thick thin film with only a real refractive index as in (a) and with additional an absorption coefficient as in (a). (c) Wavenumbers calculated from the wavelengths of the extrema of the wing spectrum of (b) fitted with the linear function Eq. 10. (d) Reflectance spectra calculated for a thin film with average thickness 730 nm and thickness varying in a Gaussian way, with full width at half maximum (FWHM) 0, 20, 40, 60, and 80 nm, together with the measured reflectance spectrum of (b) (blue curve). (e) Transmittance and reflectance spectra measured with an integrating sphere. (f) Transmittance, reflectance and absorptance spectra calculated for a thin film with thickness 730 nm, with the refractive index and absorption coefficient of (a).

amplitude decreases with decreasing wavelength. This could be due to a non-negligible absorption, and we therefore incorporated in the reflectance calculations the previously estimated absorption coefficient of insect cuticle ([12]; Fig. 4a). This reduces the oscillation amplitude in the short-wavelength range, but not at visible wavelengths.

Actually, a more obvious candidate for causing the reduced modulation is a non-constant thickness of the wing membrane. To investigate this, we calculated the averaged reflectance spectra for a thin film with thickness varying in a Gaussian way, while maintaining the average thickness 730 nm (Fig. 3d). Indeed, with increasing width of the Gaussian, the modulation of the reflectance spectrum progressively reduces. Comparing the calculated spectra with the measured spectrum indicates that the wing thickness in the measured area varies with a full width at half maximum (FWHM) of ≈40 nm (Fig. 4d). Incomplete modulations of the reflectance spectra were also encountered in the case of the mosquito wing (Fig. 3b). Most likely this result was similarly caused by slight variations in the wing thickness.

We thus conclude that insect wing membranes can be well understood with thin film optics with as specific interesting point that the local wing thickness can be estimated with a simple optical method.

Measurements on a bare wing area with an integrating sphere were largely consistent with the measurements with a bifurcated probe (Fig. 4e). The areas of illumination for the transmittance and reflectance measurements were slightly different, viz diameter ≈2 and ≈5 mm, respectively. The reflectance spectra showed less modulation, presumably because of smoothing due to a more varying thickness over a larger area. Modeling of the transmittance and reflectance for a 730 nm thick thin film with refractive index and absorption coefficient as given in Fig. 4a showed a similar but distinctly larger modulation and furthermore that absorption remains minor in the visible wavelength range.

3.3. *Damselfly wing membrane*

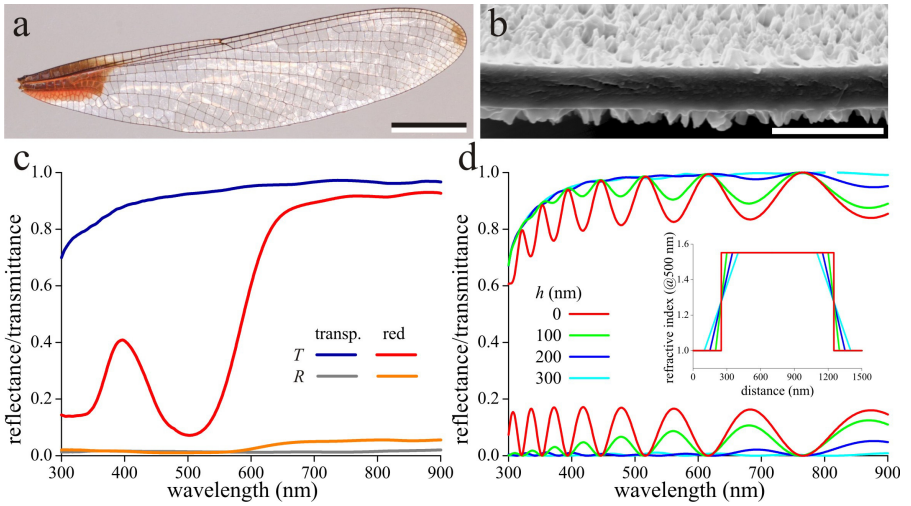

Fig. 5. Optical properties of the wing of a damselfly, the American Rubyspot, *Hetaerina americana*. (a) The wing membrane is largely colorless and transparent, but near the base, the wing is red-colored (scale bar: 5 mm). (b) Scanning electron micrograph of a sectioned wing, showing that the wing membrane is not flat, but studded with numerous small protrusions (scale bar: 5 μm). (c) Transmittance (T) and reflectance (R) spectra of a transparent and red wing area measured with an integrating sphere. (d) Transmittance and reflectance spectra calculated for a thin film with average thickness 1000 nm and refractive index and absorption coefficient as that of Fig. 4a. The refractive index was assumed to change linearly in surface layers with thicknesses h = 0, 100, 200 and 300 nm (see inset, which presents the refractive index profile at 500 nm).

The American Rubyspot, *Hetaerina americana*, is a damselfly with largely colorless, transparent wings, but near the thorax the wing has a distinct red color ([30]; Fig. 5a). Scanning electron microscopy of sectioned wings shows that the wing membrane thickness varies over the wing from below 1 μm to up to 3 μm. However, the wing membrane is not flat, but studded with numerous small protrusions, which indicates that the wing membrane may not act as an ideal, classical thin film, but rather as a plate with gradient refractive index surface layers (Fig. 5b). Indeed, the reflectance spectrum is extremely low, with minor oscillations (Fig. 5c). To understand this phenomenon, we have calculated the reflectance of a model thin film with average thickness 1000 nm and refractive index and absorption coefficient as that of Fig. 4a. The density of the thin film material was assumed to change linearly in the upper and lower surface layers with thicknesses h = 0 (ideal thin film), 100, 200 and 300 nm (see inset Fig. 5d). In the model calculations, the surface layers were approximated as consisting of a stack of 100 thin films, with thickness h/100 and with a constant refractive index, resulting in a multilayer consisting of a total of 201 thin films. The reflectance and transmittance spectra were then calculated with Eqs 5 and 6. With increasing thickness of the surface layers, the reflectance progressively diminishes. Comparing the low reflectance measured (Fig. 5c) with the modelled spectra (Fig. 5d) indicates that the membrane protrusions act as an effective impedance matching device; see also [31].

The transmittance spectra calculated for the different thin film cases similarly show decreasing oscillations with increasing height of the surface layers (Fig. 5d). At wavelengths >500 nm, the calculated reflectance and transmittance

add up to 1, but with decreasing wavelengths absorption by the cuticular pigment becomes noticeable. This is also apparent in the transmittance spectra measured from the colorless wing area (Fig. 5c). The transmittance spectra of the red wing area shows a distinct trough near 500 nm, due to (presumably) an ommochrome-type pigment [30]. Accordingly, the corresponding reflectance spectra are very low at short wavelengths, but at long wavelengths the reflectance exceeds that of the colorless area (Fig. 5c); this results from the slightly granular deposition of the pigment, causing enhanced scattering.

3.4. Butterfly wing scales

Other than the glasswing butterflies, virtually all butterflies have wings shingled with regular rows of scales, which provide the wings with often spectacular and beautiful colored patterns. The wing membrane proper has little or no color, except for the coloration due to thin film reflection effects, but as incident light first encounters the scale stacks, the wing membrane is usually unimportant for wing coloration. An exception is the swordtail butterfly *Graphium sarpedon*, where the wings have central bands with high concentrations of bile pigment, combined with carotenoids, causing a blue-green or green color (Fig. 6a; [29,32]). At the ventral wing side a remarkable type of scale occurs, with apposed upper and lower lamina, together forming a thin film with thickness ≈400 nm (Fig. 6b). These so-called glass scales are quite different from the white scales of adjacent wing patches, which have the standard structure of a flat lower lamina with an upper lamina having distinct ridges and few crossribs that line large windows (Fig. 6c).

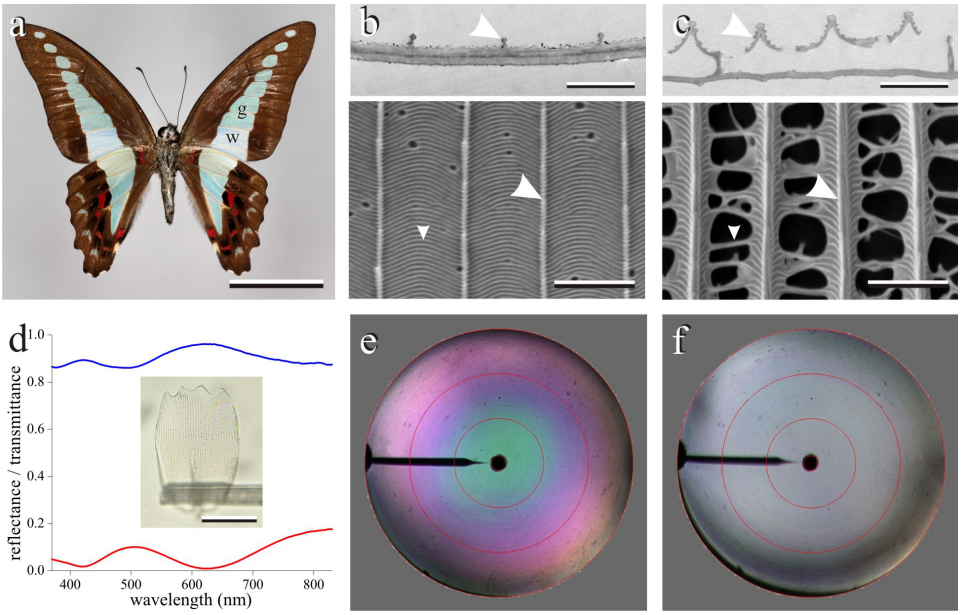

Fig. 6. Thin films of the swordtail butterfly *Graphium sarpedon*. (a) Ventral view of the wings showing colored bands surrounded with dark-brown margins. The colored patches have either unpigmented glass (g) scales or white (w) scales. (b) Transmission and scanning electron micrographs of glass scales, showing that they consist of an upper lamina, with minor ridges (large arrowhead) that are interconnected by numerous crossribs (small arrowhead), and an apposed lower lamina, together forming a thin film. (c) Micrographs of a white scale, showing a lower lamina that is similarly flat as that of the glass scale, but the upper lamina has much larger ridges and less crossribs, which leave open large windows. (d) Transmittance and reflectance spectra measured with a microspectrophotometer of a glass scale mounted at a glass pipette (inset). (e) Scatterogram of a glass scale measured with a white and wide-angled (hemispherical) illumination beam, showing the strong angle-dependence of the scale's spectral reflectance. (f) Scatterogram measured similarly of a white scale, showing its diffuse scattering.

The reflectance and transmittance spectra, measured with a microspectrophotometer, closely correspond to what is expected for a thin film with 400 nm thickness (Fig. 6d). The spectra were obtained with normal illumination, but the spectra depend strongly on the angle of incidence, as predicted by thin film theory. Upon illumination with increasing angle of light incidence, the peak reflectance shifts to shorter wavelengths. This effect can be directly visualized with an imaging scatterometer (Fig. 6e). Applying full hemispherical illumination, the scatterogram shows centrally a

green reflection, corresponding to the reflectance spectrum of Fig. 6d, but with increasing angle the reflectance shifts into the violet wavelength region (Fig. 6e). Applying the same stimulus conditions, the scatterogram of a white scale shows an overall broad-band, white reflection (Fig. 6f). Clearly the scales' disordered structure (Fig. 6c) causes diffuse white scattering [29].

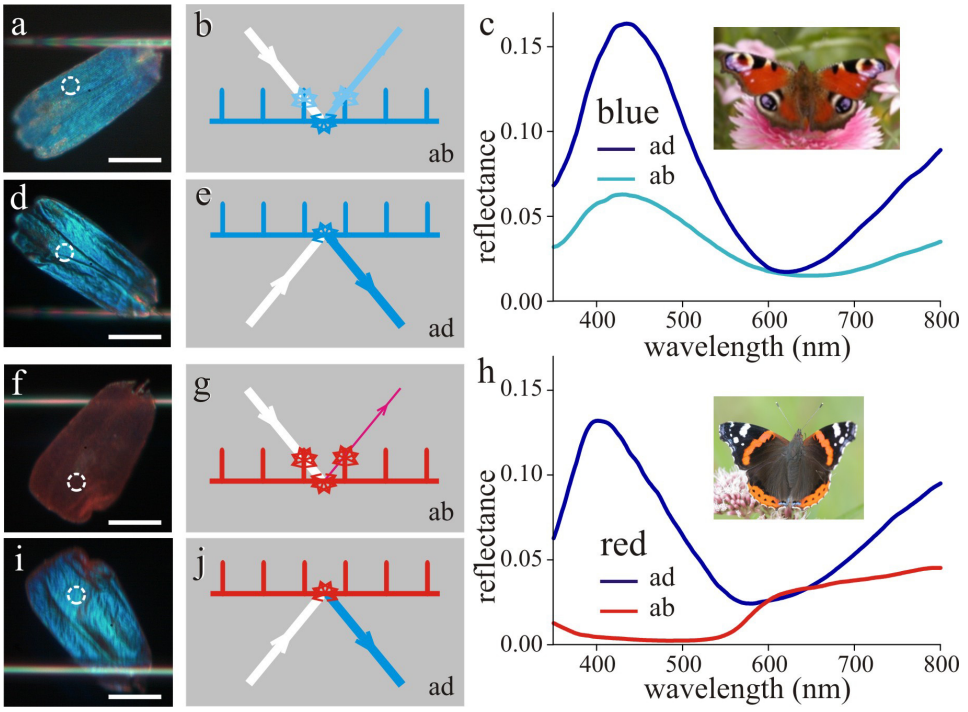

Fig. 7. Reflection properties of single nymphaline wing scales. (a-e) A blue scale from the eyespot of a Peacock butterfly, *Aglais io*. (f-h) A red scale from the red wing bands of a Red Admiral, *Vanessa atalanta*. (a, d) Photographs of the upper (abwing) and lower (adwing) sides of the blue scale. (f, i) Abwing and adwing sides of the red scale, which have a red and blue color, respectively. (b, e, g, j) Diagrams of how the thin film of the lower lamina reflects light incident from the abwing and adwing sides. (c, h) Reflectance spectra of the abwing and adwing scale sides measured from the areas indicated by dashed circles in the photographs; scale bars in (a, d, f, i): 50 μm.

The wing scales of nymphaline butterflies all have the standard structure, similar to the white scale of Fig. 6c. Surprisingly, the eyespots at the dorsal wings of the Peacock butterfly, *Aglais io*, are blue due to blue-colored scales that have at most a slight amount of melanin pigment [11]. Epi-illumination of both sides of these scales with white light yields a blue reflection (Fig. 7a,b,d,e), and both reflectance spectra measured with the microspectrophotometer are strikingly reminiscent of a thin film (Fig. 7c). Detailed analyses revealed that the lower lamina plays a dominant role in the scale's reflection properties. The spectra indicate an average thickness of ≈200 nm .

The Red Admiral butterfly, *Vanessa atalanta*, has red bands at the dorsal wings due to stacks of red colored scales. Remarkably, whereas illumination of the upper (abwing) side of these scales causes a red color, the lower (abwing) side features a distinct blue reflection (Fig. 7f,g,i,j). Clearly also in this case the lower lamina has a thickness of ≈200 nm. Transmittance measurements reveal the presence of a pigment, which strongly absorbs in the short-wavelength range [11]. With epi-illumination of the upper side, the pigment suppresses the reflection in the blue, but leaves the thin-film reflection in the long-wavelength band rather unhampered, thus causing the red color (Fig. 7g, h).

3.5. Bird feathers

Birds are covered by feathers that are often brightly colored. Exceptionally brilliant examples are male birds of paradise [24,33–35]. For instance, the male bird of paradise Lawes' parotia has in the occipital (neck) area a patch of brightly reflecting feathers [34,35]. Actually, the main part of the occipital feathers is brown, but that part is overlapped

by adjacent feathers. The distal, non-overlapped part of the feather is brightly reflecting with a distinct bluish-silvery color (Fig. 8a). The feather barbules in the distal feather area consist of ≈50 μm long elements, which are actually dead cells (Fig. 8b, lower insets). Reflectance spectra measured with a microspectrophotometer from different barbule areas have a slight peak in the blue-violet and show clear oscillations at wavelengths >600 nm, indicating thin film effects (Fig. 8b). To understand the barbules' reflection properties it is essential to know the barbule's structure as well as its refractive index profile. Anatomy revealed that the barbule elements contain highly regularly layered rodlets (Fig. 8b, upper inset). The rodlets contain melanin pigment, as followed from transmittance measurements (Fig. 8c). The transmittance is highest in a central area, the remnant of the dead cell's nucleus (see also Fig. 8b, upper inset, right side).

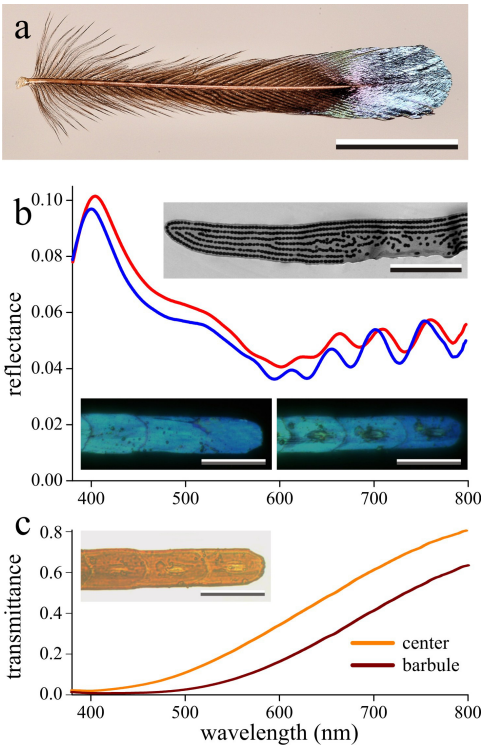

Fig. 8. Occipital feather of the bird of paradise Lawes' parotia. (a) A feather with distally very shiny barbules (scale bar: 5 mm). (b) Reflectance spectra from two small areas of an isolated barbule showing distinct oscillations at wavelengths >600 nm. Lower inset left: the barbule observed from the upper side, showing the individual barbule elements; lower inset right: the barbule observed from the underside, showing in the center of each element (cell) a reduced reflection (scale bars: 50 μm). Upper inset: transmission electron micrograph of a barbule cross-section, showing multilayers of rodlets; the layers are distorted in a central area (scale bar: 5 μm). (c) Transmittance spectra measured of the central area of a barbule element and outside this area. The spectra are characteristic for melanin pigment. Inset: the same barbule as in (b), but observed with transmitted light (scale bar: 50 μm).

The rodlets' melanin causes a higher refractive index of the rodlets compared to that of the surrounding keratin, and therefore the barbule acts as a multilayer reflector. Because the thickness of the melanin and keratin layers is ≈200 nm and the refractive indices are 1.5-1.8, the reflectance peak wavelength is in the infrared wavelength range, at ≈1.3 μm, so that the reflectance in the visible, although brightly visible, is sub-maximal [35].

The oscillations in the reflectance spectra do not arise from the multilayer, but from the total barbule acting as thin film. Applying Jamin-Lebedeff polarizing interference microscopy, we determined the refractive index of the barbules as a function of wavelength and found that its real part is well described by the Cauchy equation $n(\lambda) = A + B\lambda^{-2}$, with $A = 1.590$ and $B = 1.48\ 10^4$ nm^2 (unpublished). Together with the wavelength values of the oscillation extrema in the reflectance spectra, using Eq. 11, this yielded barbule thickness values of 3.0 ± 0.2 μm, in very good agreement with anatomical data (Fig. 8a, upper inset).

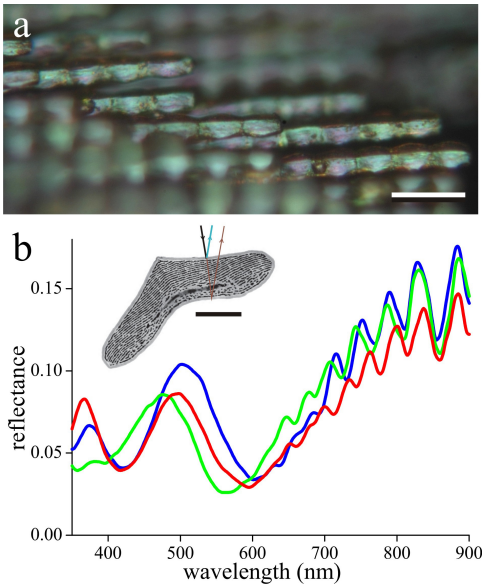

Fig. 9. Breast feather of a male Lawes' parotia. (a) Feather barbules observed while the feather was rotated 30° from its longitudinal symmetry plane (scale bar: 50 μm). (b) Reflectance spectra measured from individual barbule elements showing a main reflectance band in the blue green, due to the cortex thin film, plus oscillations at > 600 nm, due to the total barbule acting as a thin film. Inset: a cross-section of the barbule showing its boomerang shape and a cortex layer surrounding a multilayer consisting of layers of melanin rodlets embedded in keratin (scale bar: 5 μm)

Male Lawes parotia have extremely colorful breast feathers, which rapidly change colors from golden to blue to green upon slight changes in the angle of light incidence or angle of viewing [24,35]. When rotated 30° from its longitudinal symmetry plane, that is, when the birds' feather barbules are observed sideways, blue-colored reflections are seen (Fig. 9a). The reflectance spectra measured from individual barbule elements have a main peak at ≈500 nm, but distinct oscillations occur at wavelengths >600 nm (Fig. 9b). The explanation of the spectra must again be derived from the barbule fine structure. The cross-section of a breast feather barbule has a boomerang shape (Fig. 9b, inset). The interior exists, like the occipital feather barbule, of a multilayer of melanin rodlets. The multilayer is surrounded by a clear, unpigmented cortex with thickness ≈320 nm. This layer acts as a thin film, however, not facing air on both sides, which was the case for the previously treated examples. The cortex layer causes the blue peaking reflectance spectrum [24,35]. The multilayer inside the breast feather barbule consists of layers with thickness ≈120 nm, much smaller than those of the occipital feather barbules, resulting in reflectance peak wavelengths of ≈600 nm when illuminated normally in the barbule's symmetry plane [24,35].

4. Discussion

Thin film optics determines the coloration of the wings of many insects, because of the minimal thickness of the wing membrane. However, the wing membrane thickness locally varies and thus the insect wings are non-ideal thin films. We here have shown that the local average thickness can be easily determined with a simple method, by measuring reflectance spectra and then fitting a linear function to the wave numbers of the reflectance extrema (Eq. 11).

Thin film optics plays also a dominant role in the coloration of butterfly wing scales, because their lower lamina well approximates a thin film. With thicknesses of ≈200 nm, blue colored scales result, which are present in many nymphalid butterflies. When the scales contain pigments, they selectively absorb the thin film reflections of the lower lamina, when illuminated from the normal, abwing side. Illumination of the adwing side can be used to measure the reflectance spectrum of the lower lamina and thus derive its thickness. Yet, because the reflectance measurements with a microspectrophotometer on the small butterfly wing scales are necessarily done with a high power objective, and thus with a substantial aperture, the measurements must be considered with caution, as thin film spectra depend

on the angle of incidence. We have further investigated this for an ideal thin film with thickness 200 nm and with the refractive index of insect cuticle (Fig. 4a). Fig. 10a and 10b present the reflectance spectra as a function of the angle of light incidence, varying from $\phi = 0°$ to $\phi = 80°$, for TE- and TM-polarized light, respectively. The spectra show a distinct hypsochromic shift with increasing angle of light incidence. Figure 10d presents the reflectance peak wavelengths as a function of the (unidirectional) illumination angle.

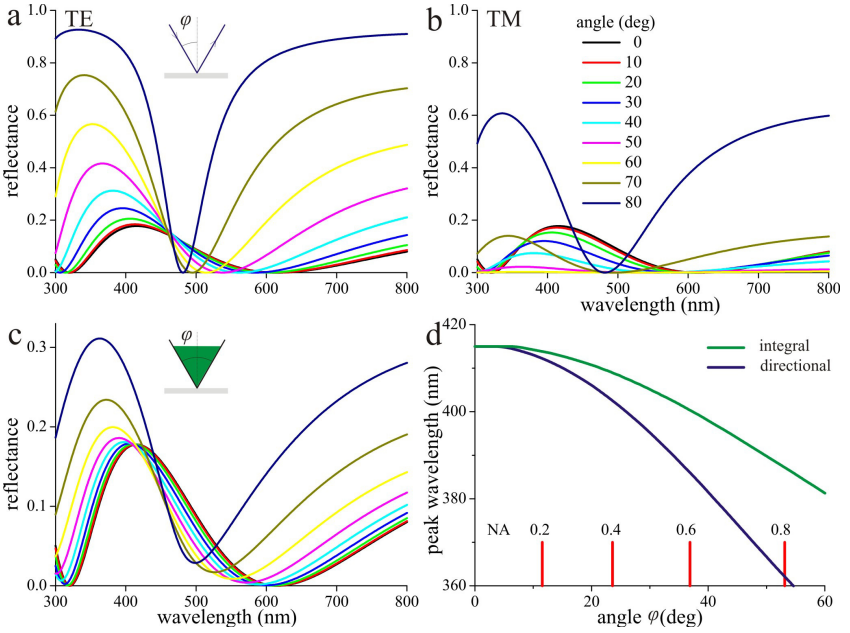

Fig. 10. Angle dependence of the reflectance spectra of a thin film with thickness 200 nm. (a) Reflectance spectra for a parallel beam of TE-polarized light with angles of incidence varying from $\phi = 0°$ to $\phi = 80°$. (b) Angle dependence of the reflectance spectra for TM-polarized light. (c) Angle dependence of the reflectance spectra for a wide-angled (integral) beam with maximal angle of incidence ϕ increasing from 0° to 80°(unpolarized light). (d) Angle dependence of the reflectance peak wavelength for parallel (directional) beams (panel a and b) and for a wide-angled (integral) beam (panel c). The numerical aperture (NA) of the integral beam, corresponding to the maximal angle of incidence, is given by the vertical bars.)

Slightly different reflectance spectra result when illumination is applied with the full aperture of the microscope objective. Figure 10c shows the reflectance spectra for illumination with unpolarised light and with varying full apertures, namely with a maximal angle of light incidence varying from $\phi = 0°$ to $\phi = 80°$; the light flux was assumed to be constant for all angular directions up to ϕ. The resulting spectra show a hypsochromic shift of the spectra with increasing aperture.

Figure 10d presents again the reflectance peak wavelengths for aperture-dependent illuminations as a function of the maximum illumination angles; the vertical bars indicate the numerical aperture (NA) of the integral beam that corresponds to the maximal angle of incidence. It follows from Figure 10d that the peak wavelengths are reliably measured with objectives having a numerical aperture < 0.2, but for numerical apertures exceeding that value corrections have to be made. The measurements with the microspectrophotometer of Figs 7-9 were performed with an objective with numerical aperture 0.45, which means that the measured peak wavelength was reduced by 2-3% with respect to the peak wavelength for normal illumination (Fig. 10d). According to Eq. 11, the thickness of a thin film then also will be underestimated by that amount.

Oscillating spectra due to thin film effects can also be measured from bird feather barbules (Fig. 8, 9) and also from the cortex of bird feather barbs [25]. The locally varying thin film thicknesses will cause averaging of the oscillations in the reflectance spectra, and then the thin film reflections will cause a spectrally flattened background signal. Nevertheless, also in this case the oscillations can be used to derive the barbule thickness.

5. Conclusion

Thin films are widely present in numerous insect and bird wings. In some cases thin film effects play a prominent role for the coloration, notably in butterfly wing scales and the breast feathers of the bird of paradise Lawes' parotia.

Acknowledgements

I thank Dr Bodo Wilts for his continuous collaboration and essential support. This study was financially supported by the Air Force Office of Scientific Research/European Office of Aerospace Research and Development AFOSR/EOARD (grant FA8655-08-1-3012).

References

[1] L. P. Biro, J.-P. Vigneron, Laser Photon Rev 5 (2011) 27–51.
[2] S. Kinoshita, Structural Colors in the Realm of Nature, Singapore: World Scientific Publishing Company, 2008.
[3] M. Srinivasarao, Chem Rev 99 (1999) 1935–1962.
[4] B. D. Wilts, K. Michielsen, J. Kuipers, H. D. Raedt, D. G. Stavenga, Proc R Soc B 279 (2012) 2524–2530.
[5] P. Vukusic, B. Hallam, J. Noyes, Science 315 (2007) 348.
[6] B. D. Wilts, K. Michielsen, H. De Raedt, D. G. Stavenga, Interface Focus 2 (2011) 681–687.
[7] L. Biró, K. Kertész, Z. Vértesy, G. Márk, Z. Bálint, V. Lousse, J.-P. Vigneron, Mat Sci Eng C 27 (2007) 941–946.
[8] E. Shevtsova, C. Hansson, D. H. Janzen, J. Kjærandsen, P Natl Acad Sci USA 108 (2011) 668–673.
[9] H. Ghiradella, In: F.W. Harrison, M. Locke (Eds.), Microscopic anatomy of invertebrates 11A: Insecta (1998) 257–287.
[10] H. Ghiradella, Adv Insect Physiol 38 (2010) 135–180.
[11] D. G. Stavenga, H. L. Leertouwer, B. D. Wilts, J Exp Biol 217 (2014) 2171–2180.
[12] D. G. Stavenga, H. L. Leertouwer, B. D. Wilts, J Comp Physiol A 200 (2014) 547–561.
[13] M. Giraldo, S. Yoshioka, D. Stavenga, J Comp Physiol A 194 (2008) 201–207.
[14] D. Stavenga, H. Leertouwer, P. Pirih, M. Wehling, Opt Express 17 (2009) 193–202.
[15] P. Vukusic, J. Sambles, C. Lawrence, R. Wootton, Proc R Soc B 266 (1999) 1403–1411.
[16] S. Yoshioka, S. Kinoshita, Proc R Soc B 273 (2006) 129–134.
[17] N. I. Morehouse, P. Vukusic, R. Rutowski, Proc R Soc B 274 (2007) 359–366.
[18] R. Rutowski, J. Macedonia, N. Morehouse, L. Taylor-Taft, Proc R Soc B 272 (2005) 2329–2335.
[19] H. L. Leertouwer, B. D. Wilts, D. G. Stavenga, Opt express 19 (2011) 24061–24066.
[20] K. J. McGraw, In: G.E. Hill, K.J. McGraw (Eds.), Bird coloration Vol. I, Mechanisms and measurements (2006) 354–398.
[21] R. O. Prum, In: G.E. Hill, K.J. McGraw (Eds.), Bird coloration Vol. I, Mechanisms and measurements (2006) 295–353.
[22] M. D. Shawkey, N. I. Morehouse, P. Vukusic, J R Soc Interface 6 (2009) S221–S231.
[23] H. Durrer, Denkschr Schweiz Naturfor Ges 91 (1977) 1–126.
[24] D. G. Stavenga, H. L. Leertouwer, N. J. Marshall, D. Osorio, Proc R Soc B 278 (2011) 2098–2104.
[25] D. G. Stavenga, J. Tinbergen, H. L. Leertouwer, B. D. Wilts, J Exp Biol 214 (2011) 3960–3967.
[26] M. Born, E. Wolf, Principles of optics, Cambridge: Cambridge University Press, 1999.
[27] D. G. Stavenga, B. D. Wilts, H. L. Leertouwer, T. Hariyama, Phil Trans R Soc B 366 (2011) 709–723.
[28] P. Yeh, Optical waves in layered media, Hoboken NJ: Wiley-Interscience, 2005.
[29] D. G. Stavenga, A. Matsushita, K. Arikawa, H. L. Leertouwer, B. D. Wilts, J Exp Biol 215 (2012) 657–662.
[30] D. G. Stavenga, H. L. Leertouwer, B. D. Wilts, Light Sci Appl 2 (2013) e100.
[31] A. Yoshida, M. Motoyama, A. Kosaku, K. Miyamoto, Zool Sci 14 (1997) 737–741.
[32] D. G. Stavenga, M. A. Giraldo, H. L. Leertouwer, J Exp Biol 213 (2010) 1731–1739.
[33] E. Scholes, Zoology 111 (2008) 260–278.
[34] E. Laman, Tim Scholes, Birds of paradise: revealing the world's most extraordinary birds, Washington DC: National Geographic, 2012.
[35] B. D. Wilts, K. Michielsen, H. D. Raedt, D. G. Stavenga, P Natl Acad Sci USA 111 (2014) 4363–4368.